# Physicochemical Evaluation of Electrospun Polyvinyl Alcohol/Keratin/Curcumin Nanofibers

You Jen Xian,[a,b] Gongtao Ding,[c] Chin Hua Chia ,[d] and Mohd Shaiful Sajab [a,b,*]

* *Corresponding author: mohdshaiful@ukm.edu.my*

*DOI: 10.15376/biores.21.4.10560-10574*

## GRAPHICAL ABSTRACT

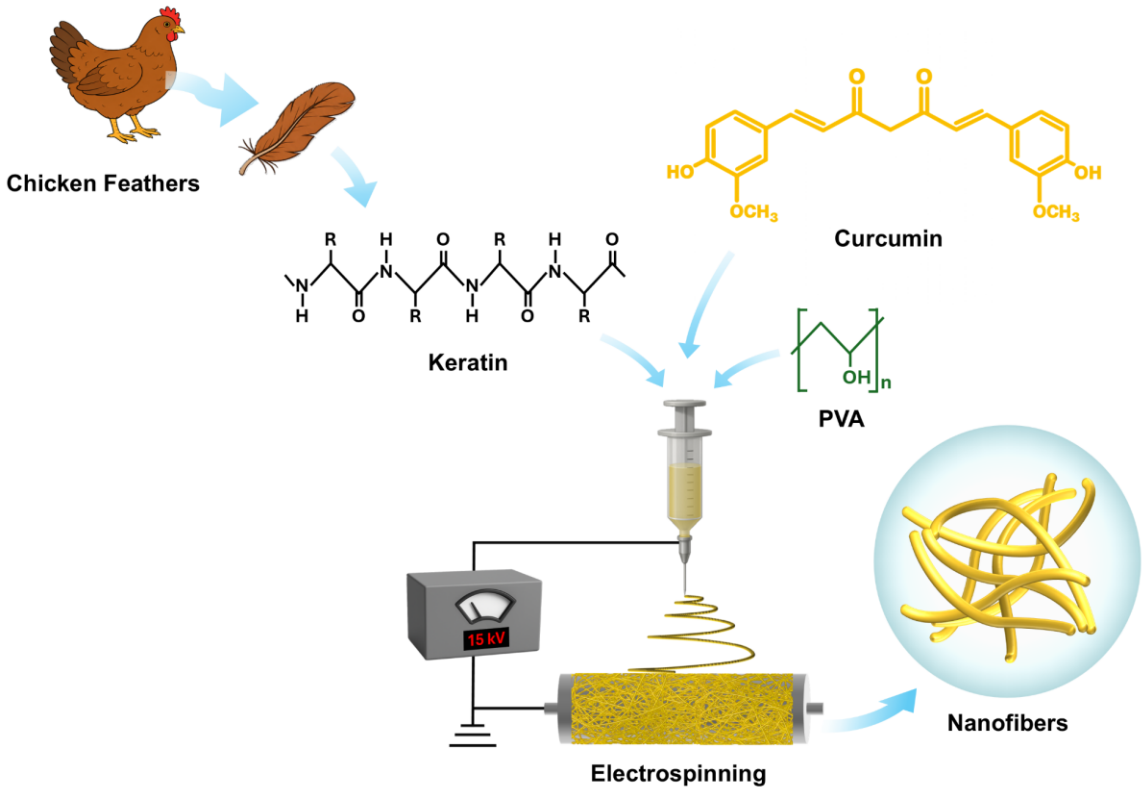

# Physicochemical Evaluation of Electrospun Polyvinyl Alcohol/Keratin/Curcumin Nanofibers

You Jen Xian,[a,b] Gongtao Ding,[c] Chin Hua Chia ,[d] and Mohd Shaiful Sajab [a,b,*]

Electrospun nanofibers have gained attention for biomedical applications due to their high surface area and extracellular matrix-like structure. In this study, polyvinyl alcohol (PVOH)-based electrospun nanofibers with keratin and curcumin were fabricated and characterized. The effects of keratin and different curcumin concentrations on morphology, chemical structure, thermal stability, wettability, and mechanical properties of the nanofibers were investigated. Field emission scanning electron microscopy (FESEM) showed that keratin incorporation noticeably reduced the fiber diameter from 453 nm to 254 nm, while increasing curcumin concentration further decreased the average fiber size from 330 nm to 282 nm. Fourier transform infrared spectroscopy (FTIR) confirmed the successful incorporation of keratin and curcumin into the nanofibers through the presence of characteristic functional groups. X-ray diffraction (XRD) analysis indicated that the nanofibers remained predominantly amorphous with the presence of crystalline curcumin domains. Differential scanning calorimetry (DSC) and thermogravimetric analysis (TGA) demonstrated improved thermal stability after the incorporation of keratin and curcumin. Water contact angle measurements revealed that all nanofibers were hydrophilic, with keratin substantially enhancing wettability. Mechanical analysis showed that keratin improved nanofiber flexibility, while curcumin influenced the balance between strength and elongation. The developed PVOH/keratin/curcumin nanofibers exhibited promising physicochemical and mechanical properties for biomedical applications.

*DOI: 10.15376/biores.21.4.10560-10574*

*Keywords: Electrospinning; Polyvinyl alcohol; Keratin; Curcumin*

*Contact information: a: Research Center for Sustainable Process Technology (CESPRO), Faculty of Engineering and Built Environment, Universiti Kebangsaan Malaysia, 43600 Bangi, Selangor, Malaysia; b: Department of Chemical and Process Engineering, Faculty of Engineering and Built Environment, Universiti Kebangsaan Malaysia, 43600 Bangi, Selangor, Malaysia; c: Key Laboratory of Biotechnology and Bioengineering of State Ethnic Affairs Commission, Biomedical Research Center, Northwest Minzu University, Lanzhou 730030, PR China; d: Materials Science Program, Faculty of Science and Technology, Universiti Kebangsaan Malaysia, Bangi, Malaysia;*
** Corresponding author: mohdshaiful@ukm.edu.my*

## INTRODUCTION

Electrospinning is a versatile and straightforward technique that is widely used for the fabrication of nanofibers with high surface area, interconnected porous structures, and tuneable physicochemical properties (Liu *et al.* 2020; Zulkifli *et al.* 2023). These characteristics have made electrospun nanofibers attractive for a wide range of applications, including wound dressings, tissue engineering, drug delivery, filtration, and biomedical devices. Among various polymers for electrospinning, polyvinyl alcohol (PVOH) has received considerable attention because of its excellent spinnability, water

solubility, ability to form film, and biocompatibility. In addition, the presence of abundant hydroxyl groups in PVOH enables intermolecular interactions with other functional materials, making it suitable for polymer blending systems (Rao Kotni *et al.* 2023; Yavari *et al.* 2025). However, neat PVOH nanofibers possess limited functionality and are highly sensitive to aqueous environments. Therefore, incorporating bio-based materials is required to tailor their structural and physicochemical properties for advanced applications.

Natural proteins have emerged as useful materials for electrospun polymer systems because of their biodegradability, biocompatibility, and diverse functional groups. Keratin is a natural fibrous protein that is abundantly available from poultry feather waste. The utilization of feather-derived keratin not only provides an environmentally sustainable approach for converting a waste stream but also offers a renewable biomaterial for advanced functional materials. Keratin chemically contains abundant amino ($-NH_2$), carboxyl (-COOH), and hydroxyl (-OH) groups, which can readily form hydrogen bonds with the hydroxyl groups of PVOH. Such intermolecular interactions are expected to affect the structural and functional properties of electrospun nanofibers. The incorporation of keratin into PVOH systems has been reported to influence the physicochemical and mechanical properties of the resulting materials (He *et al*. 2017; Jung *et al*. 2021).

Curcumin is a natural polyphenolic compound extracted from turmeric and has been extensively studied in electrospun nanofiber systems (de Oliveira *et al*. 2020; Sharifi-Rad *et al*. 2020). This is mainly due to its antioxidant, antibacterial, and anti-inflammatory properties, which make it attractive for applications, such as wound dressing, tissue engineering, and drug delivery (Tamilarasi *et al.* 2022; You *et al.* 2026). Due to its rigid molecular structure and partially crystalline nature, curcumin may modify polymer chain organization, crystallinity, thermal behavior, wettability, and mechanical properties depending on its concentration and dispersion within the electrospinning solution (Sun *et al.* 2013; Priyadarsini 2014; Snetkov *et al.* 2022).

Recent studies have demonstrated the successful incorporation of keratin and turmeric-derived compounds into electrospun polymer nanofibers for functional applications. For example, Petrai *et al.* (2025) fabricated electrospun PVOH/κ-carrageenan membranes coated with curcumin *via* electrospraying and reported enhanced antibacterial activity, good cytocompatibility, and promising wound-healing performance. More recently, Clerici *et al.* (2026) developed electrospun pectin/PVOH nanofibers containing bioactive keratin hydrolysates and turmeric, demonstrating composition-dependent changes in morphology, thermal stability, mechanical properties, antioxidant activity, and antimicrobial performance for active food packaging applications. However, the individual and combined effects of keratin incorporation and curcumin concentration on fiber morphology, intermolecular interactions, crystallinity, thermal behavior, wettability, and mechanical performance have not yet been fully established.

Based on the properties of each material, the incorporation of keratin and curcumin was expected to modify the intermolecular interactions within the PVOH matrix, thereby affecting fiber morphology, structural organization, and the physicochemical properties of the electrospun nanofibers. Keratin, with its abundant amino, carboxyl, and hydroxyl functional groups, was expected to interact with PVOH through hydrogen bonding (Fig. 1). Meanwhile, curcumin was anticipated to influence the structural organization of the nanofibers because of its rigid molecular structure and partially crystalline nature. Therefore, this study aimed to investigate the influence of keratin incorporation and varying curcumin concentrations to the morphology, physicochemical, thermal and mechanical properties of electrospun PVOH-based nanofibers. The outcomes of this study

are expected to provide useful insights for the development of sustainable polymer-based nanofiber materials.

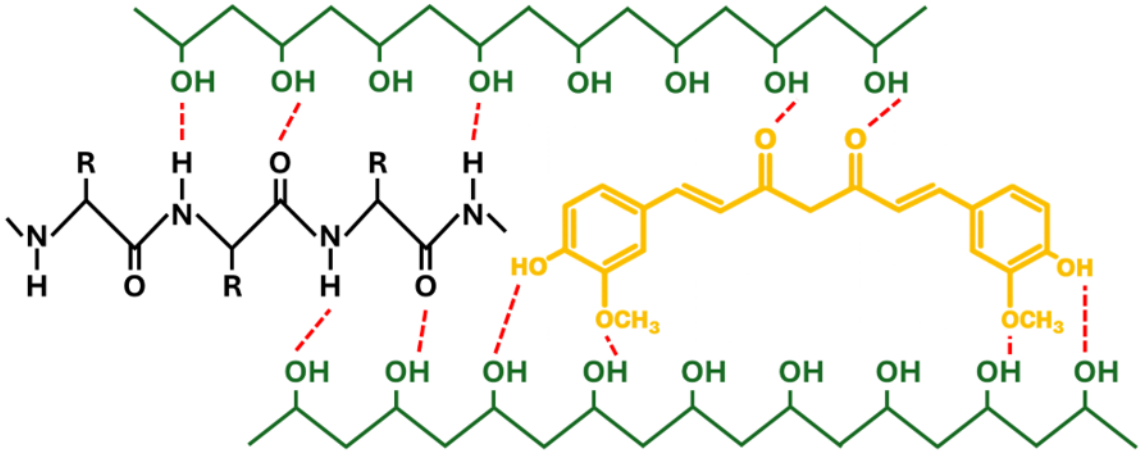


**Fig. 1.** Schematic illustration of the intermolecular interactions among PVOH, keratin, and curcumin

## EXPERIMENTAL

### Materials

Polyvinyl alcohol (PVOH; alcoholysis 98~99% mol/mol) and sodium persulfate were obtained from Macklin (Shanghai, China). Curcumin (> 97%) was obtained from TCI Chemicals (Tokyo, Japan). Sodium hydroxide (NaOH) and urea were purchased from Shanghai Hushi Chemical Reagent (Shanghai, China). Sodium dodecyl sulfate (SDS) was from Solarbio (Beijing, China).

### Extraction of Keratin

Chicken feathers were first washed and dried. After that, 30 g chicken feathers were mixed with sodium persulfate, SDS, and urea at weight ratios of 1:0.5, 1:1, and 1:8, respectively. These ratios were selected based on preliminary optimization experiments conducted prior to this study. Distilled water was then added to dissolve the mixture completely. The pH of the solution was adjusted to 11 using NaOH to facilitate keratin solubilization under alkaline conditions before extraction in a water bath at 80 °C for 12 h. After cooling to room temperature, the extracted solution was centrifuged at 5,000 rpm for 10 min to separate insoluble residues. The resulting supernatant was collected and subjected to dialysis against distilled water for 5 days, followed by freeze-drying to obtain keratin powder.

### Preparation of Electrospun Nanofibers

A 6 wt% PVOH solution was prepared by dissolving PVOH in distilled water using a water bath at 90 °C until a clear homogeneous solution was obtained. To minimize water evaporation during heating, the beaker was covered with aluminium foil throughout the preparation process. For the preparation of PVOH/keratin/curcumin solutions, 0.5 wt% keratin powder and curcumin at different concentrations (0.25, 0.5, 0.75, and 1 wt%) were added to the prepared PVOH solution under continuous magnetic stirring. The nanofibers

were fabricated using an electrospinning process at a feed rate of 0.01 mL/min with an applied voltage of 15 kV. A 19 G needle was used, and the distance between the needle tip and the drum collector was maintained at 15 cm.

## Characterization

*Field emission scanning electron microscopy (FESEM) and fiber diameter measurement*

The morphology and fiber diameter of the electrospun nanofibers were analyzed using field emission scanning electron microscopy (FESEM; SU8220, Hitachi, Tokyo, Japan) at magnifications corresponding to scale bars of 500 nm and 10 μm. Before imaging, the samples were mounted onto aluminium stubs using carbon tape and sputter-coated with a thin gold layer for 60 s. Average fiber diameters were determined by measuring 100 random fibers from three FESEM images using ImageJ software.

*Fourier transform infrared spectroscopy (FTIR)*

Fourier transform infrared spectroscopy (FTIR; Nicolet iS10, Thermo Fisher Scientific, Waltham, MA, USA) equipped with an attenuated total reflectance (ATR) accessory was used to identify the chemical structure of the electrospun nanofibers without further sample preparation. For keratin powder, FTIR analysis was performed using the KBr pellet method. Spectra were recorded over the range of 4000 to 500 $cm^{-1}$ with a resolution of 4 $cm^{-1}$ and 32 accumulated scans per sample.

*X-ray diffraction (XRD)*

X-ray diffraction (XRD) analysis was performed using a diffractometer (Empyrean, Malvern Panalytical, Almelo, Netherlands). The diffraction patterns were collected over a $2\theta$ range of 10° to 70° at a scanning rate of 5°/min.

*Thermal analyses*

For thermal characterization, approximately 5 mg of each sample was sealed in an aluminum pan for differential scanning calorimetry (DSC; 204 F1, NETZSCH, Selb, Germany). A similar amount was placed in a crucible for thermogravimetric analysis (TGA; STA 449 F5, NETZSCH, Selb, Germany). The DSC measurements were conducted from 10 to 300 °C at a heating rate of 10 °C/min, whereas TGA measurements were performed from 25 °C to 600 °C at the same heating rate. All thermal analyses were performed under a constant nitrogen flow rate of 50 mL/min.

*Water contact angle measurement*

The surface wettability of the electrospun scaffolds was evaluated using a contact angle meter (V5, Yunfan Technology, Tianjin, China). A 3 μL droplet of deionized water was deposited onto the sample surface, and the water contact angle was recorded. Measurements were conducted at three different locations for each sample.

*Mechanical analysis*

Mechanical properties were determined using a universal testing machine (AI-3000, GOTECH, Taichung, Taiwan) equipped with a 200 N load cell at room temperature. The specimens were prepared with dimensions of 10 mm × 50 mm and tested at a crosshead speed of 5 mm/min until fracture occurred.

*Statistical analysis*

Statistical analysis was performed using OriginPro 2024 software, and all data were expressed as mean ± SD (n = 3). One-way analysis of variance (ANOVA) followed by Tukey's post hoc test was used to determine significant differences among formulations. Differences were considered statistically significant at $p < 0.05$.

## RESULTS AND DISCUSSION

### Morphological Characterization of Electrospun Nanofibers

The surface morphology and fiber diameter of the electrospun nanofibers were examined to evaluate the effects of adding keratin and curcumin on fiber formation. As shown in Fig. 2, all formulations showed bead-free nanofibers, indicating a successful and stable electrospinning process.

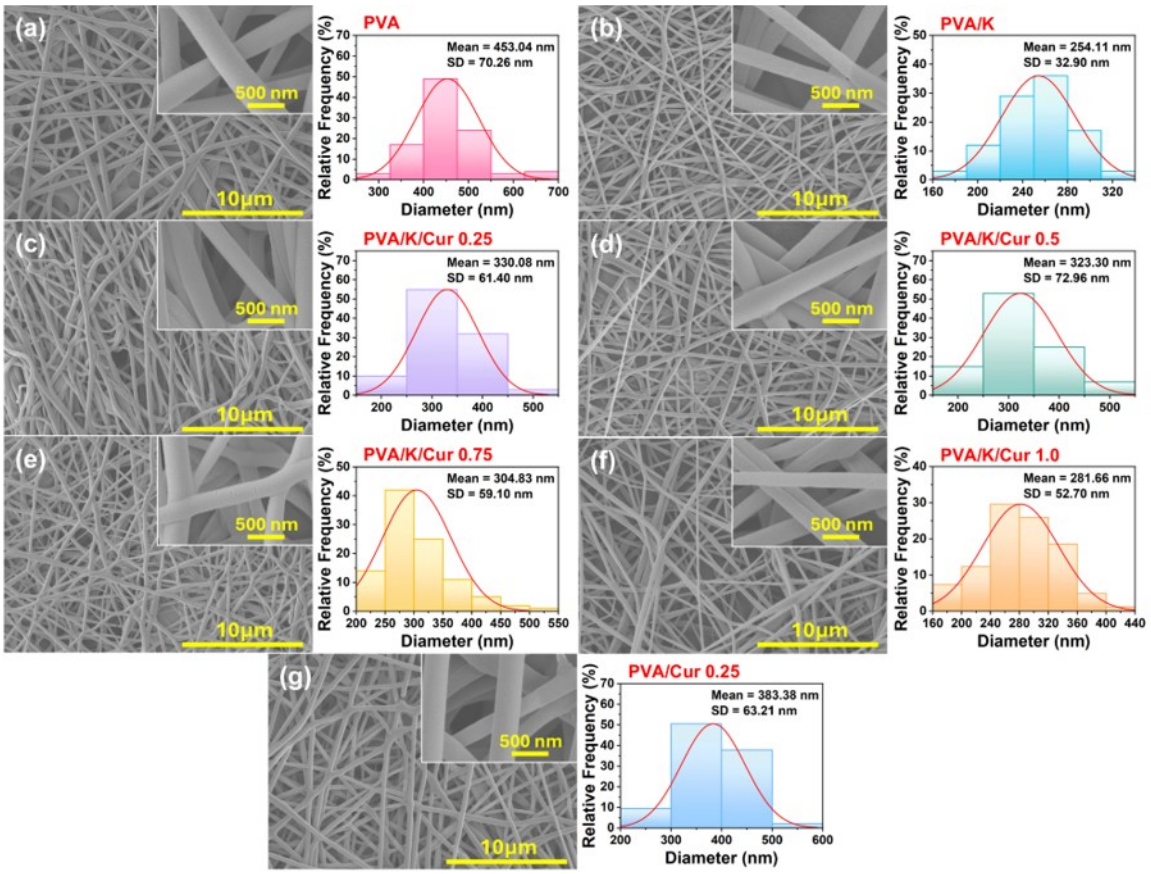


**Fig. 2.** FESEM micrographs and fiber diameter distributions of (a) PVOH, (b) PVOH/K, (c) PVOH/K/Cur 0.25, (d) PVOH/K/Cur 0.5, (e) PVOH/K/Cur 0.75, (f) PVOH/K/Cur 1.0, and (g) PVOH/Cur 0.25

Electrospun neat PVOH (Fig. 2(a)) showed smooth fibers with the largest average diameter of 453.04 ± 70.26 nm. After incorporating keratin (Fig. 2(b)), the fiber diameter significantly decreased to 254.11 ± 32.90 nm. This may be caused by the decreased viscosity of the spinning solution after keratin incorporation, which facilitated greater stretching of the polymer jet during electrospinning and resulted in thinner fibers (Nezarati *et al.* 2013).

In the PVOH/K/Cur system, as the curcumin concentration increased from 0.25% to 1.0%, the average fiber diameter gradually decreased from 330.08 ± 61.40 nm (Fig. 2(c)) to 281.66 ± 52.70 nm (Fig. 2(f)). This may be attributed to increased charge density or changes in solution conductivity at higher curcumin concentrations (Chen *et al.* 2010; Sun *et al.* 2013). The effects promoted stronger elongation of the electrospinning jet and resulted in finer fibers. Similar trends were also reported in previous studies on PLA/curcumin and PVOH/curcumin nanofibers (Chen *et al.* 2010; Sun *et al.* 2013). In contrast, the electrospun PVOH/Cur 0.25 without keratin (Fig. 2(g)) exhibited a much larger fiber diameter than PVOH/K/Cur 0.25, suggesting that keratin played an important role in reducing fiber diameter and improving fiber uniformity. The formation of finer and more uniform nanofibers is desirable because it provides a higher surface area and a more homogeneous fibrous structure, which contributes to more consistent physicochemical properties. Interestingly, Clerici *et al.* (2026) reported homogeneous electrospun pectin/PVOH nanofibers containing keratin hydrolysates and turmeric with fiber diameters ranging from 405 to 518 nm. Meanwhile, keratin incorporation in the present PVOH-based system resulted in a noticeable reduction in fiber diameter. The differences between the studies may be attributed to variations in formulation composition, including the use of a PVOH/pectin matrix and turmeric in the previous study, compared with the PVOH matrix and pure curcumin used in the present work.

## Chemical and Thermal Analyses of Electrospun Nanofibers

As shown in Fig. 3(a), the FTIR spectrum of electrospun neat PVOH exhibited characteristic absorbance bands of PVOH functional groups. The most notable feature was the broad band around 3277 $cm^{-1}$, which corresponded to the hydroxyl (O-H) stretching vibration (Yang *et al.* 2021). The peaks at 2940 and 2911 $cm^{-1}$ were attributed to the asymmetric and symmetric stretching vibrations of aliphatic C-H groups in the polymer backbone (Yang *et al*. 2021; Nguyen *et al.* 2026). The absorbance band at 1711 $cm^{-1}$ was assigned to the carbonyl (C=O) stretching vibration of residual acetate groups in PVOH (Al-Emam *et al.* 2020). Meanwhile, the peaks located at 1420 $cm^{-1}$ and 1330 $cm^{-1}$ were attributed to $CH_2$ bending and C-H wagging vibrations, respectively (Arango *et al.* 2024). In the fingerprint region, the strong peak at 1088 $cm^{-1}$ was assigned to C-O stretching vibrations. Additionally, the bands at 919 and 838 $cm^{-1}$ corresponded to $CH_2$ rocking and C-C stretching vibrations, respectively (Arango *et al.* 2024; Martínez-Vela *et al.* 2026).

Extracted keratin displayed an absorbance band around 3300 $cm^{-1}$ corresponding to the amide A band, which was attributed to N-H and O-H stretching vibrations (Sharma *et al.* 2018; Mattiello *et al.* 2022). The peaks observed at 2919 and 2851 $cm^{-1}$ corresponded to the asymmetric and symmetric stretching vibrations of C-H groups, respectively. In addition, the characteristic amide bands also appeared in the spectrum. The absorbance bands at 1655, 1545, and 1223 $cm^{-1}$ were assigned to the amide I (C=O stretching), amide II (N-H bending and C-N stretching), and amide III (C-N stretching and N-H bending) bands, respectively (Sharma *et al.* 2018). Among the characteristic keratin bands, only the amide I region (1655 $cm^{-1}$) showed a slight increase in absorbance in the keratin-containing nanofibers compared with neat PVOH. In contrast, no noticeable changes were observed in the amide II and amide III regions, which may be associated with the relatively low keratin content in the formulation and intermolecular hydrogen-bonding interactions between PVOH and keratin.

Curcumin-loaded nanofibers showed several additional absorbance bands that were absent in both electrospun neat PVOH and keratin spectra. The peaks at 1628 $cm^{-1}$ and

1603 $cm^{-1}$ were associated with conjugated C=O and aromatic C=C stretching vibrations of curcumin, respectively (Teixeira *et al.* 2015). Meanwhile, the band at 1509 $cm^{-1}$ corresponded to aromatic ring vibrations. Furthermore, the band at 1027 $cm^{-1}$ was related to C-O-C stretching vibrations (Espinoza-Torres *et al.* 2023). These peaks confirmed the presence of curcumin within the curcumin-loaded nanofibers.

The XRD analysis was conducted to examine the crystallinity and structural changes of the electrospun PVOH nanofibers after incorporating keratin and curcumin. Figure 3(b) shows a broad diffraction peak at $2\theta = 20.98°$ for electrospun neat PVOH, which is the characteristic of its semi-crystalline nature (Chandra *et al.* 2025). These results suggest that the keratin was acting as a plasticizing agent. This plasticizing behavior is fully consistent with both the crystalline and molecular nature of the extracted protein. Structurally, XRD analysis revealed that the characteristic α-helix and β-sheet diffraction attributes of pure keratin at approximately $2\underline{\theta} = 11.24°$ and 21.28° and disappear within the PVOH/K blend (Alahyaribeik and Ullah 2020; Ahmed Zim *et al.* 2026). For the curcumin-loaded nanofibers, a sharp diffraction peak was seen at around $2\theta = 17.26°$, which corresponded to the crystalline structure of curcumin (Chen *et al.* 2018). Meanwhile, the broad diffraction halo around 20 to 22° suggests that the overall structure was still predominantly amorphous despite the presence of crystalline curcumin domains.

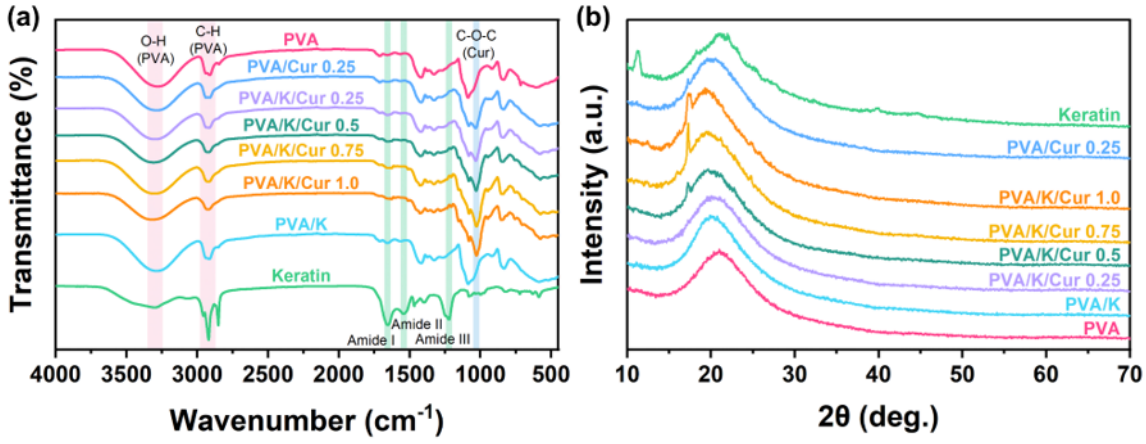


**Fig. 3.** Chemical characterization of extracted keratin and electrospun PVOH-based nanofibers: (a) FTIR spectra and (b) XRD patterns

The DSC method was used to evaluate the thermal behavior and intermolecular interactions of the electrospun PVOH-based nanofibers following the incorporation of keratin and curcumin. The DSC thermograms are presented in Fig. 4(a), while the corresponding melting temperatures ($T_m$) are summarized in Table 1. First, all nanofibers exhibited a broad endothermic transition centered around 70 to 100 °C, which is attributed to the loss of absorbed and bound moisture. Neat PVOH nanofibers displayed a pronounced melting peak at 221.2 °C, corresponding to the melting of the semi-crystalline regions of PVOH. The incorporation of keratin (PVOH/K) slightly increased the melting temperature to 223.2 °C. This suggests the presence of intermolecular interactions, particularly hydrogen bonding between the hydroxyl groups of PVOH and the functional groups of keratin, which may have strengthened the crystalline regions of the electrospun nanofibers. Similar findings have been reported for PVOH/collagen films (Sionkowska *et al.* 2010).

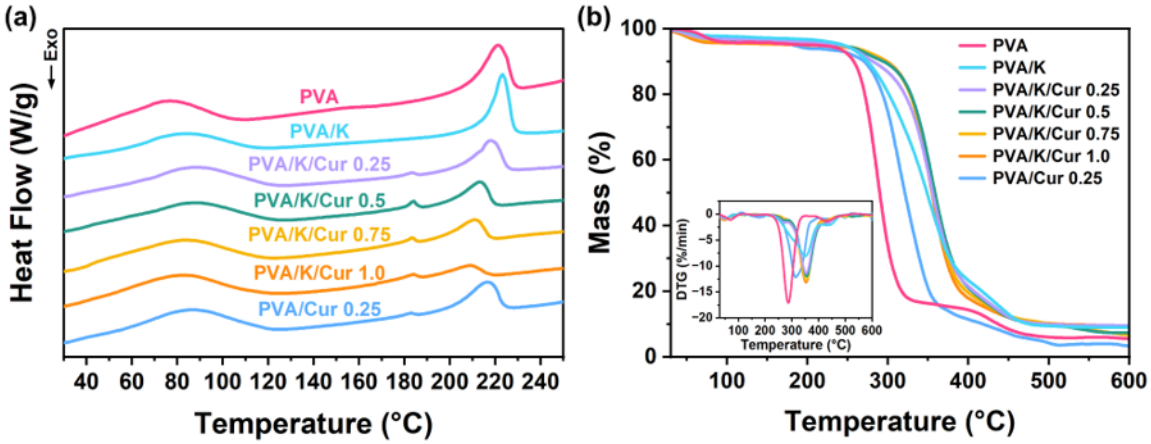


**Fig. 4.** (a) DSC thermograms and (b) TGA and DTG curves of the electrospun nanofibers

**Table 1.** Thermal Properties of Electrospun Nanofibers

| Electrospun Nanofibers | $T_{m,\ PVOH}$ (°C) | $T_{m,\ Cur}$ (°C) | $T_{onset}$ (°C) | $T_{max}$ (°C) |
|---|---|---|---|---|
| PVOH | 221.2 | - | 265.4 | 287.1 |
| PVOH/K | 223.2 | - | 288.1 | 351.2 |
| PVOH/K/Cur 0.25 | 218.2 | 183.2 | 316.4 | 353.5 |
| PVOH/K/Cur 0.5 | 214.2 | 184.2 | 322.2 | 354.8 |
| PVOH/K/Cur 0.75 | 212.2 | 183.2 | 320.9 | 354.1 |
| PVOH/K/Cur 1.0 | 209.2 | 184.2 | 322.0 | 352.8 |
| PVOH/Cur 0.25 | 217.3 | 182.3 | 285.7 | 312.6 |

Compared with neat PVOH, all curcumin-containing nanofibers exhibited lower melting temperatures, ranging from 209.2 to 218.2 °C. In addition, the melting temperature of PVOH gradually reduced as curcumin concentration increased, from 218.2 °C for PVOH/K/Cur 0.25 to 209.2 °C for PVOH/K/Cur 1.0. Similarly, PVOH/Cur 0.25 also exhibited a lower melting temperature of 217.3 °C. This trend suggests that curcumin influenced the melting behavior of the PVOH matrix by modifying its crystalline arrangement. The incorporation of curcumin may have disrupted the regular packing of PVOH chains, resulting in a lower melting temperature. However, the additional diffraction peaks observed in the XRD patterns indicate the presence of crystalline curcumin within the nanofibers. This suggests that the reduction in melting temperature was associated with changes in the crystalline arrangement of the PVOH matrix rather than an overall reduction in the crystallinity of the nanofibers. For the curcumin-loaded nanofibers, additional endothermic peaks were observed at approximately 182.3 to 184.2 °C. They were attributed to the melting temperature of curcumin (Mankan *et al.* 2025). These thermal transitions indicate the presence of crystalline curcumin within the nanofibers. The observation is consistent with the XRD results, where characteristic diffraction peaks of curcumin were detected.

The TGA and DTG analyses were performed to determine the effect of keratin and curcumin on thermal degradation behavior and thermal stability of the electrospun nanofibers. From Fig. 4(b), all nanofibers showed initial weight loss below approximately 150 °C. This is attributed to the removal of absorbed and bound moisture from the nanofiber structure. Electrospun neat PVOH showed a major thermal degradation stage between approximately 250 and 350 °C. From Table 1, neat PVOH exhibited the lowest onset degradation temperature ($T_{onset}$ = 265.4 °C) and maximum degradation temperature

($T_{max}$ = 287.1 °C), indicating the lowest resistance to thermal degradation among all fabricated nanofibers.

The addition of keratin into the PVOH system increased both $T_{onset}$ and $T_{max}$, which indicate enhanced thermal stability of the nanofibers. This improvement may be attributed to the formation of hydrogen-bonding interactions between the hydroxyl groups of PVOH and the carboxyl and amide groups of keratin (Habib *et al.* 2025). These intermolecular interactions restricted the mobility of the polymer chains during thermal treatment, thereby delaying thermal degradation. Furthermore, all PVOH/K/Cur nanofibers displayed a similar thermal degradation trend with higher degradation temperatures. They showed $T_{onset}$ values in the range of 316.4 °C to 322.2 °C and $T_{max}$ values between 352.8 °C and 354.8 °C. Although the incorporation of curcumin reduced the melting temperature observed in the DSC analysis, the higher $T_{onset}$ and $T_{max}$ values indicate improved thermal stability of the nanofibers. The further improvement may be attributed to the presence of benzene rings and conjugated double bonds in curcumin, which enhance the structural stability and delay the thermal breakdown of the nanofibers (Teng *et al.* 2025). In comparison, PVOH/Cur 0.25 nanofibers exhibited lower thermal stability than the PVOH/K/Cur nanofibers, with $T_{onset}$ and $T_{max}$ values of 285.7 and 312.6 °C, respectively. This observation shows that the combination of both keratin and curcumin provided greater thermal stabilization than curcumin alone.

## Physical and Mechanical Analyses of Electrospun Nanofibers

Surface wettability of the electrospun nanofibers was identified with water contact angle measurement, as shown in Fig. 5(a). All fabricated nanofibers displayed water contact angle values below 90°, which indicate their hydrophilic nature. The water contact angle of neat PVOH nanofibers was 36.60°, which corresponded to hydroxyl groups present in the PVOH structure.

The incorporation of keratin significantly increased the hydrophilicity of the nanofibers, with the significantly lower water contact angle of 16.43° (***$p < 0.001$) compared with neat PVOH. This may be due to the presence of hydrophilic functional groups in keratin such as amino and carboxylic groups, which promoted stronger interactions between the surface of nanofibers and water molecules (Wu *et al.* 2018). In addition, the reduced fiber diameter and improved fiber uniformity observed after keratin incorporation may have further contributed to the enhanced wettability by providing a higher surface area for water interaction.

For the PVOH/K/Cur series, the values were between 17.53° and 22.53°. Only minor statistical differences were observed among the PVOH/K/Cur formulations, indicating that curcumin concentration had only a limited influence on the wettability of the keratin-containing nanofibers. This result shows that the hydrophilicity of PVOH and keratin remained dominant within the nanofiber system despite the incorporation of curcumin. The slight increase in water contact angle for some samples may be due to the hydrophobic nature of curcumin, which partially reduced the surface affinity toward water. In contrast, PVOH/Cur 0.25 nanofibers exhibited a significantly higher water contact angle of 35.97° than the PVOH/K/Cur nanofibers (**$p < 0.01$ or ***$p < 0.001$), which was comparable to neat PVOH. This observation suggests that the absence of keratin reduced the overall hydrophilicity of the nanofibers, further demonstrating the combined influence of keratin chemistry and morphology on nanofiber wettability.

The mechanical properties of the electrospun nanofibers were presented in Fig. 5(b)-(d) and Table 2. Among the nanofibers, neat PVOH nanofibers exhibited the highest

tensile strength and modulus with values of 20.3 MPa and 1076.6 MPa, respectively. It also showed moderate flexibility with an elongation at break of 50.7%. After incorporating keratin, the elongation at break increased significantly to 104.4% (*** $p < 0.001$), which indicates enhanced flexibility and ductility. Meanwhile, the tensile strength and modulus decreased significantly to 14.5 MPa (**$p < 0.01$) and 183.5 MPa (***$p < 0.001$), respectively. This mechanical behavior directly correlates with the structural and thermal characteristics observed in our prior analyses. As shown in the DSC results (Table 1), the melting temperature of PVOH slightly increased, confirming that the crystalline domains were not disrupted but rather stabilized by intermolecular hydrogen bonds. When co-spun, these disordered protein backbones lose their characteristic α-helix and β-sheet crystalline domains (broad XRD peaks at $2\theta$ = 11.24 and 21.28°) and molecularly disperse between the polymer strands. Therefore, the simultaneous reduction in stiffness and dramatic increase in ductility are attributed to a plasticizing effect of keratin within the amorphous regions of the PVOH network, which enhances chain mobility and free volume.

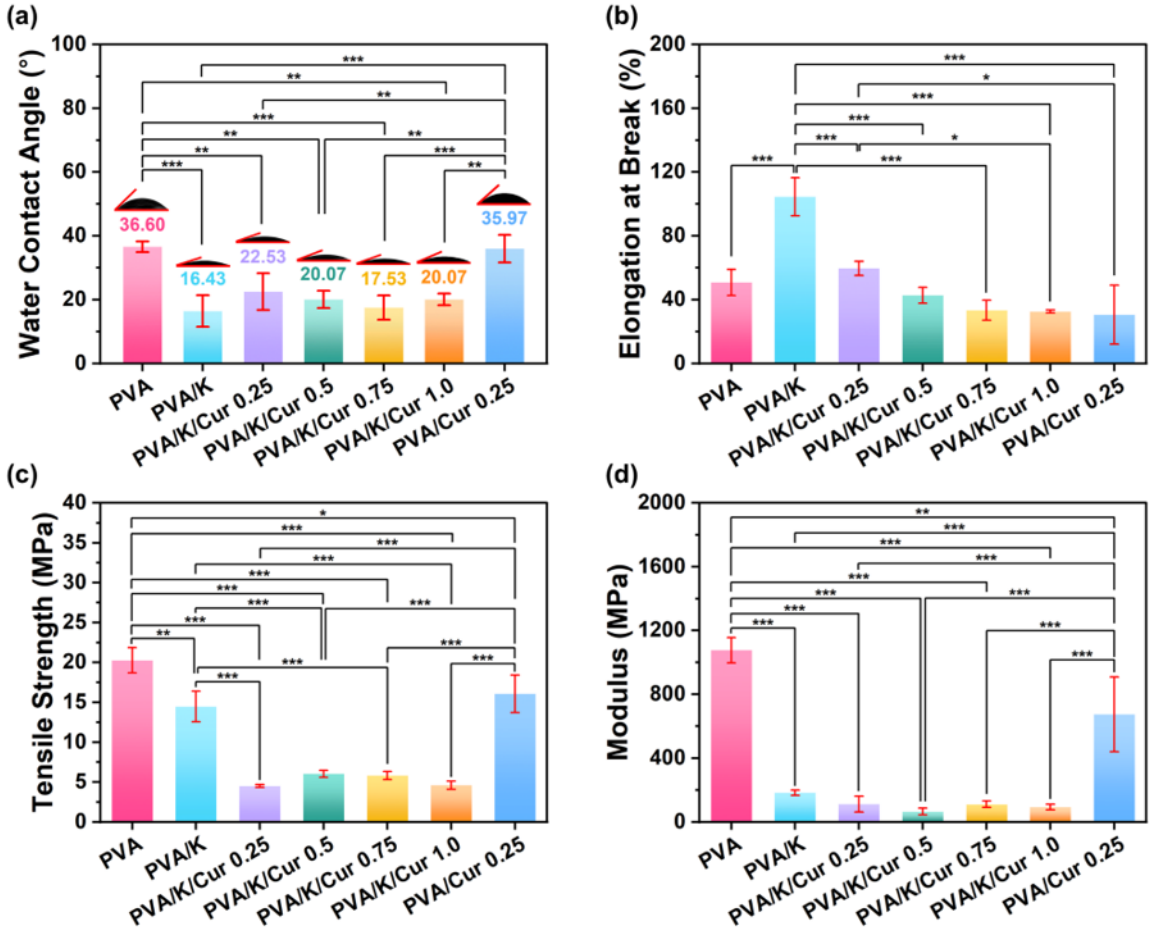


**Fig. 5.** (a) Water contact angle, (b) elongation at break (%), (c) tensile strength (MPa), and (d) Young's modulus (MPa) of the electrospun nanofibers. Data are presented as mean ± SD (n = 3), *$p < 0.05$, **$p < 0.01$ and ***$p < 0.001$

In the PVOH/K/Cur series, the elongation at break gradually decreased with increasing curcumin concentration, from 59.6% for PVOH/K/Cur 0.25 to 32.5% for PVOH/K/Cur 1.0. All PVOH/K/Cur formulations exhibited significantly lower elongation

at break than PVOH/K (***$p < 0.001$), indicating that curcumin incorporation reduced the flexibility of the nanofibers. Similarly, all PVOH/K/Cur formulations exhibited significantly lower tensile strength than both neat PVOH and PVOH/K (***$p < 0.001$). This may be due to crystalline curcumin domains within the nanofiber structure, which affected the continuity and packing arrangement of the polymer chains. Curcumin addition may have disrupted stress transfer efficiency within the polymer network and reduce mechanical stability of the nanofibers. Among the curcumin-loaded samples, PVOH/K/Cur 0.5 and PVOH/K/Cur 0.75 showed slightly higher tensile strength, suggesting that moderate curcumin incorporation may help in partial reinforcement of the nanofiber structure. However, excessive curcumin loading appeared to negatively affect the mechanical performance of the nanofibers.

Compared to the PVOH/K/Cur nanofibers, PVOH/Cur 0.25 showed significantly higher tensile strength and modulus but lower elongation at break. This suggests that the absence of keratin led to a stiffer but less flexible nanofiber structure. Overall, the incorporation of keratin improved the flexibility of the electrospun nanofibers. Meanwhile, curcumin influenced the balance between flexibility and mechanical strength depending on its concentration within the polymer system.

**Table 2.** Tensile Properties of Electrospun Nanofibers at Room Temperature

| Electrospun Nanofibers | Elongation at Break (%) | Max. Tensile Stress (MPa) | Modulus (MPa) |
|---|---|---|---|
| PVOH | 50.73 ± 8.20 | 20.26 ± 1.58 | 1076.63 ± 78.95 |
| PVOH/K | 104.45 ± 11.94 | 14.48 ± 1.92 | 183.47 ± 16.63 |
| PVOH/K/Cur 0.25 | 59.56 ± 4.42 | 4.52 ± 0.16 | 111.45 ± 50.19 |
| PVOH/K/Cur 0.5 | 42.69 ± 4.97 | 6.03 ± 0.44 | 64.85 ± 20.95 |
| PVOH/K/Cur 0.75 | 33.36 ± 6.22 | 5.82 ± 0.51 | 111.01 ± 19.88 |
| PVOH/K/Cur 1.0 | 32.52 ± 0.96 | 4.60 ± 0.50 | 93.01 ± 17.26 |
| PVOH/Cur 0.25 | 30.58 ± 18.45 | 16.06 ± 2.34 | 674.45 ± 233.93 |

## CONCLUSIONS

1. This study demonstrated the feasibility of converting feather-derived keratin, an abundant agricultural by-product, into a functional additive for tailoring the physicochemical properties of electrospun polyvinyl alcohol (PVOH) nanofibers. The findings highlight a sustainable approach for value-added utilization of feather waste while providing insights into how natural protein incorporation can be used to regulate nanofiber characteristics.
2. The incorporation of keratin significantly influenced the physicochemical properties of the electrospun PVOH nanofibers by producing finer and more uniform fibers, enhancing wettability and flexibility, and improving thermal stability. These results demonstrate the multifunctional role of feather-derived keratin in modifying the performance of electrospun nanofibers through intermolecular interactions within the polymer matrix.
3. Curcumin incorporation further tailored the physicochemical properties of the electrospun nanofibers in a concentration-dependent manner. The presence of crystalline curcumin domains influenced the thermal behavior, wettability, and mechanical performance of the nanofibers, demonstrating that curcumin concentration

can be used to regulate the overall characteristics of the electrospun PVOH/keratin nanofiber system.

4. Among the fabricated formulations, PVOH/K/Cur 0.5 exhibited the most balanced overall physicochemical performance by combining the highest thermal stability and tensile strength among the curcumin-containing nanofibers while maintaining excellent hydrophilicity. Therefore, PVOH/K/Cur 0.5 may serve as a suitable reference formulation for future studies on PVOH/keratin/curcumin electrospun nanofibers.

## ACKNOWLEDGMENTS

The authors gratefully acknowledge the financial and technical support provided by the Ministry of Science, Technology and Innovation (MOSTI), Malaysia through the grant provided under Technology Development Fund 2 (TeD 2) [grant number TEF08241295].

### Conflict of Interest

The authors declare that they have no known competing financial interests or personal relationships that could have appeared to influence the work reported in this paper.

### Use of Generative AI

During the preparation of this work, the authors used ChatGPT to improve language and readability. After using this tool, the authors have reviewed and edited the content as needed and take full responsibility for the content of the publication.

## REFERENCES CITED

Ahmed Zim, M. K., Hashem, M. A., Hasan Zahin, M. E., Hassan, A., and Miem, M. M. (2026). "Synthesis of hydroxyapatite-keratin nanocomposites for chromium adsorption from tannery wastewater," *Water Resources and Industry* 35, article 100339. https://doi.org/10.1016/J.WRI.2025.100339

Alahyaribeik, S., and Ullah, A. (2020). "Methods of keratin extraction from poultry feathers and their effects on antioxidant activity of extracted keratin," *International Journal of Biological Macromolecules* 148, 449-456. https://doi.org/10.1016/J.IJBIOMAC.2020.01.144

Al-Emam, E., Soenen, H., Caen, J., and Janssens, K. (2020). "Characterization of polyvinyl alcohol-borax/agarose (PVA-B/AG) double network hydrogel utilized for the cleaning of works of art," *Heritage Science* 8(1), article 106. https://doi.org/10.1186/S40494-020-00447-3

Arango, M. C., Jaramillo-Quiceno, N., Badia, J. D., Cháfer, A., Cerisuelo, J. P., and Álvarez-López, C. (2024). "The impact of green physical crosslinking methods on the development of sericin-based biohydrogels for wound healing," *Biomimetics* 9(8), article 497. https://doi.org/10.3390/BIOMIMETICS9080497

Chandra, J. P., Thakur, K., Uthra, D., and Hashim, A. (2025). "Design and fabrication of tailored Dy2O3 PVA nanocomposites with optical characterization for advanced

optoelectronic applications," *Scientific Reports* 15(1), article 32905. https://doi.org/10.1038/s41598-025-16535-y

Chen, J., Qin, X., Zhong, S., Chen, S., Su, W., and Liu, Y. (2018). "Characterization of curcumin/cyclodextrin polymer inclusion complex and investigation on its antioxidant and antiproliferative activities," *Molecules* 23(5), article 1179. https://doi.org/10.3390/MOLECULES23051179

Chen, Y., Lin, J., Fei, Y., Wang, H., and Gao, W. (2010). "Preparation and characterization of electrospinning PLA/curcumin composite membranes," *Fibers and Polymers* 11(8), 1128-1131. https://doi.org/10.1007/S12221-010-1128-Z

Clerici, N. J., Helm Júnior, R., Corrêa, A. N. R., Vencato, A. A., Juchem, A. L. M., Rolla, H. C., Daroit, D. J., and Brandelli, A. (2026). "Pectin/poly(vinyl alcohol) nanofibers incorporating turmeric and keratin hydrolysates: Innovative biomaterials with multifunctional properties," *International Journal of Biological Macromolecules* 373, article 153067. https://doi.org/10.1016/J.IJBIOMAC.2026.153067

de Oliveira, M. C. A., da Silva, F. A. G., da Costa, M. M., Rakov, N., and de Oliveira, H. P. (2020). "Curcumin-loaded electrospun fibers: Fluorescence and antibacterial activity," *Advanced Fiber Materials* 2(5), 256-264. https://doi.org/10.1007/S42765-020-00048-6

Espinoza-Torres, S., López, R., Sotomayor, M. D. P. T., Tuesta, J. C., Picasso, G., and Khan, S. (2023). "Synthesis, characterization, and evaluation of a novel molecularly imprinted polymer (MIP) for selective quantification of curcumin in real food sample by UV-Vis spectrophotometry," *Polymers* 15(16), article 3332. https://doi.org/10.3390/POLYM15163332/S1

Habib, M. L., Munshi, M. H., Kamruzzaman, M., Baul, T., and Hasan, M. M. (2025). "Synthesis and characterization of polyvinyl alcohol-based bioplastic film incorporated with keratin extracted from duck feathers," *Results in Materials* 27, article 100735. https://doi.org/10.1016/J.RINMA.2025.100735

He, M., Zhang, B., Dou, Y., Yin, G., Cui, Y., and Chen, X. (2017). "Fabrication and characterization of electrospun feather keratin/poly(vinyl alcohol) composite nanofibers," *RSC Advances* 7(16), 9854-9861. https://doi.org/10.1039/C6RA25009B

Jung, S., Pant, B., Climans, M., Curtis Shaw, G., Lee, E. J., Kim, N., and Park, M. (2021). "Transformation of electrospun Keratin/PVA nanofiber membranes into multilayered 3D Scaffolds: Physiochemical studies and corneal implant applications," *International Journal of Pharmaceutics* 610, article 121228. https://doi.org/10.1016/J.IJPHARM.2021.121228

Liu, Z., Ramakrishna, S., and Liu, X. (2020). "Electrospinning and emerging healthcare and medicine possibilities," *APL Bioengineering* 4(3), article 30901. https://doi.org/10.1063/5.0012309

Mankan, E., Sagdic, O., and Karadag, A. (2025). "Development and characterization of spray-dried curcumin–lecithin complexes with improved solubility and *in vitro* digestive and thermal stability," *Foods* 14(18), article 3157. https://doi.org/10.3390/FOODS14183157

Martínez-Vela, L. de J., Montero-Cortés, M. I., Qui-Zapata, J. A., Farias-Cervantes, V. S., López-Velázquez, J. C., Chávez-Rodríguez, A. M., Barba-Godínez, J. M., and García-Carvajal, Z. Y. (2026). "Gelatin–chitosan–PVA hydrogels incorporating trichoderma and their application in the control of phytopathogens," *Gels* 12(2), article 144. https://doi.org/10.3390/GELS12020144

Mattiello, S., Guzzini, A., Del Giudice, A., Santulli, C., Antonini, M., Lupidi, G., and Gunnella, R. (2022). "Physico-chemical characterization of keratin from wool and chicken feathers extracted using refined chemical methods," *Polymers* 15(1), article 181. https://doi.org/10.3390/POLYM15010181

Nezarati, R. M., Eifert, M. B., and Cosgriff-Hernandez, E. (2013). "Effects of humidity and solution viscosity on electrospun fiber morphology," *Tissue Engineering. Part C: Methods* 19(10), article 810. https://doi.org/10.1089/TEN.TEC.2012.0671

Nguyen, T. D., Nguyen, M. D., Nguyen, M. P., Vo, H. P., Nguyen, D. S., Phan, T. L., and Nguyen, T. C. (2026). "Fabrication and interfacial characterization of rGO/CS/PVA nanocomposite films for enhanced food preservation," *Results in Surfaces and Interfaces* 23, article 100769. https://doi.org/10.1016/J.RSURFI.2026.100769

Petrai, N., Loukelis, K., and Chatzinikolaidou, M. (2025). "Curcumin-functionalized electrospun nanofibrous membranes with antimicrobial activity for wound healing," *Nanomaterials* 15(5), article 388. https://doi.org/10.3390/NANO15050388

Priyadarsini, K. I. (2014). "The chemistry of curcumin: From extraction to therapeutic agent," *Molecules* 19(12), article 20091. https://doi.org/10.3390/MOLECULES191220091

Rao Kotni, T., Pandey, S., Shekhar, S., Ranjan, R., and Sarthi Srivastava, P. (2023). "Synthesis of PVA nano fibers by using electrospinning," *Materials Today: Proceedings* 80, 1158-1161. https://doi.org/10.1016/J.MATPR.2022.12.124

Sharifi-Rad, J., Rayess, Y. El, Rizk, A. A., Sadaka, C., Zgheib, R., Zam, W., Sestito, S., Rapposelli, S., Neffe-Skocińska, K., Zielińska, D., *et al.* (2020). "Turmeric and its major compound curcumin on health: Bioactive effects and safety profiles for food, pharmaceutical, biotechnological and medicinal applications," *Frontiers in Pharmacology* 11, article 01021. https://doi.org/10.3389/FPHAR.2020.01021

Sharma, S., Gupta, A., Kumar, A., Kee, C. G., Kamyab, H., and Saufi, S. M. (2018). "An efficient conversion of waste feather keratin into ecofriendly bioplastic film," *Clean Technologies and Environmental Policy* 20(10), 2157-2167. https://doi.org/10.1007/s10098-018-1498-2

Sionkowska, A., Płanecka, A., Kozłowska, J., and Skopińska-Wiśniewska, J. (2010). "Study on the thermal properties of poly(vinyl alcohol) in the presence of collagen," *Copernican Letters* 1, article 112. https://doi.org/10.12775/CL.2010.016

Snetkov, P., Morozkina, S., Olekhnovich, R., and Uspenskaya, M. (2022). "Electrospun curcumin-loaded polymer nanofibers: solution recipes, process parameters, properties, and biological activities," *Materials Advances* 3(11), 4402-4420. https://doi.org/10.1039/D2MA00440B

Sun, X.-Z., Williams, G. R., Hou, X.-X., and Zhu, L.-M. (2013). "Electrospun curcumin-loaded fibers with potential biomedical applications," *Carbohydrate Polymers* 94(1), 147-153. https://doi.org/10.1016/j.carbpol.2012.12.064

Tamilarasi, G. P., Krishnan, M., Sabarees, G., Gouthaman, S., Alagarsamy, V., and Solomon, V. R. (2022). "Emerging trends in curcumin embedded electrospun nanofibers for impaired diabetic wound healing," *Applied Nano* 3(4), 202–232. https://doi.org/10.3390/APPLNANO3040015

Teixeira, C. C. C., Mendonça, L. M., Bergamaschi, M. M., Queiroz, R. H. C., Souza, G. E. P., Antunes, L. M. G., and Freitas, L. A. P. (2015). "Microparticles containing curcumin solid dispersion: Stability, bioavailability and anti-inflammatory activity," *AAPS PharmSciTech* 17(2), article 252. https://doi.org/10.1208/S12249-015-0337-6

Teng, D. Y., Xue, Y. F., Chen, Z. Y., Wang, Y. R., and Jiang, G. C. (2025). "Preparation and performance testing of curcumin-based polyurethane materials," *Polymer Bulletin* 82(8), 2827-2844. https://doi.org/10.1007/S00289-025-05651-4

Wu, P., Dai, X., Chen, K., Li, R., and Xing, Y. (2018). "Fabrication of regenerated wool keratin/polycaprolactone nanofiber membranes for cell culture," *International Journal of Biological Macromolecule* 114, 1168-1173. https://doi.org/10.1016/J.IJBIOMAC.2018.03.157

Yang, X., Wang, B., Sha, D., Liu, Y., Liu, Z., Shi, K., Liu, W., Yu, C., and Ji, X. (2021). "PVA/poly(hexamethylene guanidine)/gallic acid composite hydrogel films and their antibacterial performance," *ACS Applied Polymer Materials* 3(8), 3867-3877. https://doi.org/10.1021/ACSAPM.1C00447

Yavari, A., Ito, T., Yamazoe, E., Hara, K., and Tahara, K. (2025). "PVA nanofibers: Electrospinning techniques and pharmaceutical applications," *Therapeutic Delivery* 16(11), 1071-1093. https://doi.org/10.1080/20415990.2025.2582465

You, J. X., Chia, K. S., Chia, C. H., Ding, G., and Sajab, M. S. (2026). "Evaluation of blended and dual-nozzle electrospun PLA/PBS nanofibers for hydrophobic drug adsorption–desorption behaviour," *Journal of Materials Science* 61, 16126-16139.

Zulkifli, M. Z. A., Nordin, D., Shaari, N., and Kamarudin, S. K. (2023). "Overview of electrospinning for tissue engineering applications," *Polymers* 15(11), article 2418. https://doi.org/10.3390/POLYM15112418

Article submitted: May 26, 2026; Peer review completed: June 27, 2026; Revised version received: July 10, 2026; Accepted: August 10, 2026; Published: September 12, 2026.
DOI: 10.15376/biores.21.4.10560-10574